Use of radar data to unveil the paleolakes and the ancestral course of Wadi El-Arish, Sinai Peninsula, Egypt

Mostafa AbuBakr [a,*], Eman Ghoneim [b], Farouk El-Baz [a], Mahmoud Zeneldin [c], Salah Zeid [d]

[a] Center for Remote Sensing, Boston University, 725 Commonwealth Avenue, Boston, MA 02155, USA
[b] Department of Geography and Geology, University of North Carolina, Wilmington, 601 S. College Rd, Wilmington, MA 28403, USA
[c] Geology Department, Al-Azhar University, Nasr City, Cairo, Egypt
[d] Geology Department, Al-Azhar University, Assiut, Egypt

ARTICLE INFO

ABSTRACT

Aspects of the geomorphic evolution of Wadi El-Arish, the largest ephemeral drainage system in the Sinai Peninsula, are still ambiguous, and its paleochannels remain undefined. One of the obstacles that impede recognition of these paleodrainage features is the variation in topography from past to present. Some of this variation is attributable to the post Miocene tectonic activity in the region. This activity might have continued to the present, and led to developing an alternative course for the paleoriver. The folded Syrian Arc Belt in North Sinai had a significant influence on the shape and direction of Wadi El-Arish. Anticlinal ridges appear to have formed natural barriers that blocked the water flow across the main drainage course during humid periods, and forced Wadi El-Arish to deviate from its original course. In this research, we attempt to reconstruct the structural deformation and simulate the paleotopography to understand the evolution of the paleodrainage systems of the region. The unique perspective offered by space-borne radar data was used to define the structurally controlled paleolakes along Wadi El-Arish and to trace its former course. With a length of 109 km, the former main channel course of Wadi El-Arish was depicted west of Gebel Halal. Three major paleolakes were defined within structurally controlled depressions. The largest lake occupied an area of at least 337 km^2 and contained approximately 10.7 km^3 of water when filled during pluvial phases. The simulation of the paleotopography was confirmed by field observations, and led to a concept for improved management of the renewable water resources in the study area. Thus, a 2 km long canal with a depth of 6 m is recommended to be established within the structural uplift. This canal would redirect the occasional runoff to a vast flat area west of Gebel Halal to provide water for approximately 1400 km^2 of fertile land for agricultural development. The flow redirection would also help to mitigate the negative effects of flash floods in El-Arish City and maximize the harvesting of rain water that would otherwise be lost to the sea.

1. Introduction

The Egyptian Sinai Peninsula is an extension of the Great Sahara (Fig. 1), which is among the driest deserts on Earth, where rainfall is less than 40 mm yr^{-1} (Sultan et al., 2011). However, the geologic evidence indicates that the Eastern Sahara had undergone climatic fluctuations of wet and dry pluvial episodes during the Quaternary (Szabo et al., 1995; Ghoneim et al., 2012). The last major wet cycle occurred during the Holocene (9500–4500 yr BP; Sultan et al., 2011). Wadi El-Arish is one of the ephemeral rivers that were active during these wet phases concurrent with the adjacent paleodrainge systems of the Eastern Sahara (El-Baz et al., 1998). At present, the tributaries of Wadi El-Arish are dry, channeling the occasional flash flood northward over the central carbonate plateau of Sinai, toward the Mediterranean Sea at El-Arish City (Fig. 1). Although northeastern Sinai receives

the largest amount of rainfall in Egypt (~304 mm yr^{-1}; Mills and Shata, 1989), demand of freshwater resources is still impeding sustainable development in Sinai. Wadi El-Arish has the largest watershed (22,600 km^2) in the Sinai and collects over 60% of the peninsula's precipitation (Abubakr et al., 2010). Hence, it has been chosen for the present study to provide a practical solution for sustainable agricultural development in North Sinai, based on the renewable runoff and the potential groundwater of its paleolakes.

Although many authors have investigated the geomorphology and hydrology of North Sinai (e.g., Shata, 1959, 1960; Diab and Himida, 1981; El-Ghazawi, 1989; Mills and Shata, 1989; Smith et al., 1997; Sultan et al., 2011), only a few studies focused on the formation process of the ancestral course of Wadi El-Arish and its associated paleolakes (e.g., El-Baz et al., 1998; Kusky and El-Baz, 2000). These studies mostly relied upon the optical satellite images (Landsat MSS and TM). For example, El-Baz et al. (1998) proposed the formation of longitudinal paleolakes along the main river course of Wadi El-Arish during humid climatic phases that ended around 10–5 ka. They justified

* Corresponding author. Tel.: +1 617 353 5981; fax: +1 617 353 2000.
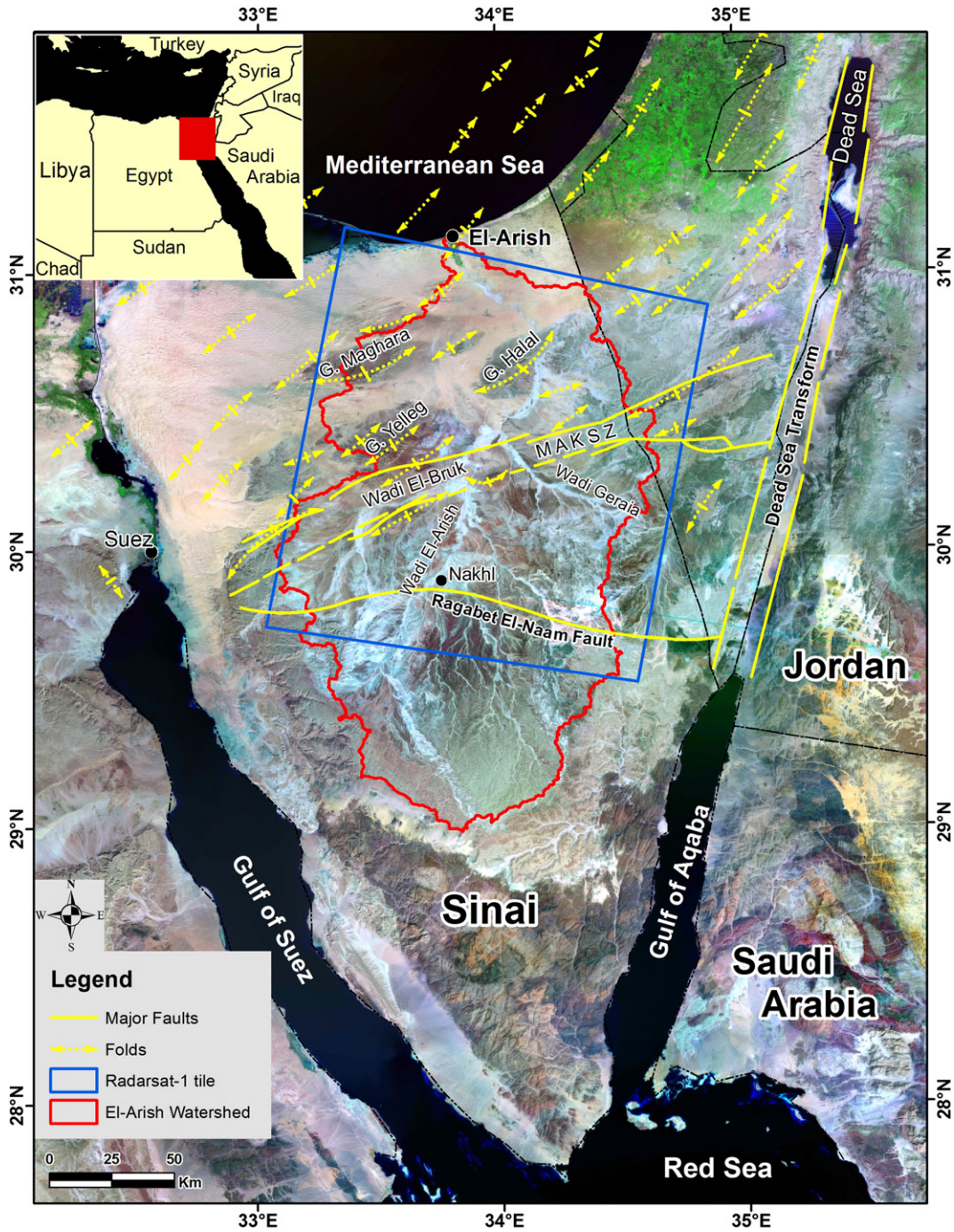 E-mail address: mostafa@bu.edu (M. AbuBakr).

Fig. 1. Landsat image mosaic (ETM + bands 7, 4 and 2) showing the location of the EL-Arish watershed (red enclosure) and the major structural features of North Sinai (modified after Jenkins, 1990). Note the parallelism of the main wadi tributaries to the major structural trends. The blue box shows the location of the Radarsat-1 image in Fig. 2.

their assumption by the presence of highly reflective salt layer along the wadi bed that is clearly visible in the Landsat images (Fig. 1).

Many earlier studies (Bar-Yousef and Phillips, 1977; Sneh, 1982; Goldberg, 1984) correlated the blocked former drainage of Wadi El-Arish with the migratory sand dunes. Kusky and El-Baz (2000), on the other hand, attributed such blocked drainage with folds and faults in the region, but without specifying the structural deformation that caused the stream deviation. The goal of the present work is to use remote sensing and geographic information systems (GIS) to de-lineate the former shape and flow direction of Wadi El-Arish before recent uplifting, and explain the causes that led it to deviate from its original course. This study also aims to map paleolakes along the

former river course and estimate the amount of water held in the lakes. A broad impact of this study would include establishing an approach that integrates recent remote sensing data, geomorphology and geological structure to understand the paleodrainge evolution and its implications on groundwater potentiality, which could be ap-plied elsewhere in arid lands.

2. The study area

The Sinai Peninsula is a micro-plate wedged between the African and Arabian plates within the hyper-arid desert belt (Said, 1990). This triangular territory is bounded by major tectonics and structural

trends, which significantly influenced the shape and direction of its drainage patterns. Therefore, most of the reaches of Wadi El-Arish are parallel to or follow the major structural trends in Sinai (El-Baz et al., 1998). For instance, the upper reaches of Wadi El-Arish in Nakhl City are parallel to the NE–SW structural trend of the Gulf of Aqaba–Dead Sea Transform (Fig. 1). To the east, Wadi Geraia follows extensional faults parallel to the Gulf of Suez rift system (Kusky and El-Baz, 1998). Wadi El-Bruk, south of Gebel Yelleg, occupies the southern flank of synclinal fold and tends ENE–WSW, parallel to the Minshera Abu-Kandu Shear Zone (MAKSZ in Fig. 1; Mills and Shata, 1989).

In the northern Sinai, particularly north of the E–W striking Ragabet El-Naam fault, the structures become more complex. The Syrian Arc Fold Belt (Krenkel, 1925; Youssef, 1968; Said, 1990; Kusky and El-Baz, 2000) stretches as rugged isolated hills of doubly plunging anticlinal folds called Gebel (herein referred to as G., e.g., G. Yelleg, G. Halal and G. Maghara) (Fig. 1). These ridges have axial surfaces striking NE–SW, probably due to the tectonic activity associated with the rotation of the Sinai and Arabia around a pole centered near Cairo (Le Pichon and Gaulier, 1988). The carbonates of Jurassic through Cretaceous are affected by the Syrian folding system, which began in the Santonian and ended by the Eocene for the most part (Bosworth et al., 1999). However, it is documented by evidences that uplifting deformation has continued to the present (Ambraseys and Barazangi, 1989; Chaimov et al., 1992; Barazangi et al., 1996; Kusky and El-Baz, 2000), as elucidated by historical earthquakes and recent seismicity (Kebeasy, 1990). In addition, further evidence suggests that the fold belt has been recently uplifted, and subsequent erosion has not had enough time to form wide flat-bottomed wadis (Holbrook and Schumm, 1999). These anticlinal ridges appear to have formed natural dams that obstructed the stream course of Wadi El-Arish during pluvial periods. Accordingly, several temporary paleolakes developed behind the folded ridges and extended 4 to 10 km along the main channel. The river thus deviated from its original course, and pushed its water overload through three gorges, 150 to 500 m wide (Fig. 2a). The flow followed the predominant fault plains that trend in NE–SW and NW–SE directions through carbonate anticlines to the Mediterranean Sea.

3. Data and methodology

Due to the hyper-arid climate and the dry soil in the study area, the space-borne radar images represent powerful tools for recognizing paleodrainage features (Ghoneim et al., 2012). Therefore, the Radarsat-1 and the Shuttle Radar Topography Mission (SRTM) provided the basic data for this research (Figs. 2b, d and 3). Optical satellite images by the Landsat ETM+ (Fig. 2a, c; http://earthexplorer.usgs.gov/) and the high-resolution images of GeoEye and Spot 5 satellites aggregated in Google-Earth (http://www.google.com/earth) were also used as supplementary data. The optical data were employed for visual interpretation of surface features and paleolake sediments (Fig. 2a). All the aforementioned data were projected on the Universal Transverse Mercator (UTM) with WGS84 datum in GIS for further correlation of features.

3.1. Radarsat-1

The present work employed the standard mode of Radarsat-1, an Earth observation satellite developed by the Canadian Space Agency (Parashar et al., 1993). It carried a synthetic aperture radar (SAR) C-band sensor that collects data in a descending orbit at a single frequency, and wavelength of 5.8 cm horizontally (HH) polarized with 12.5 m pixel spacing. The short wavelength of C-band is useful for discriminating buried features up to 0.5 m deep (Schaber et al., 1997). C-band data have been used by many researchers to reveal paleochannels and paleolakes in Eastern Sahara (e.g., McCauley et al.,

1982; Robinson et al., 2006; Ghoneim and El-Baz, 2007a; Paillou et al., 2009; Ghoneim et al., 2012).

In this research, Radarsat-1 data were used to unveil the ancestral course of Wadi El-Arish and confirm the suggested scenarios for its evolution based on the reconstruction of paleotopography. The main stream channel of Wadi El-Arish is covered by one Radarsat-1 scene (Fig. 1), acquired on 18-Nov-2000 with an incidence angle of 35.085°.

The raw SAR image was geocoded and resampled to the same pixel size of the Landsat ETM+ panchromatic band 8 (14.25 m) using the ENVI 4.8 software package. The cubic resampling method was applied for the image transformation process using 50 ground control points (GCPs) with RMS error less than 0.6 pixels. These points are well distributed in the flat wadi deposits to avoid the topographic distortion of layover, foreshortening, and shadow effects in hilly areas. The SAR image was enhanced using the Lee filter with a kernel size of 7×7 to reduce inherent speckles and improve the image for interpretation.

The enhanced radar image (Fig. 2b) was interpreted based on the radar backscatter coefficient, which is particularly sensitive to changes in surface roughness and dielectric constant (Lee et al., 2011). This fact has been used to reveal information about surface roughness, grain size and moisture content. Since radar low backscatter indicates flat regions with dry smooth texture of fine deposits, it would appear dark owing to specular reflection of the radar wave away from the receiving antenna, whereas high backscatter represents a rugged area with coarse deposits or rocky surfaces, and would appear bright because of diffuse reflection (Jensen, 2000).

3.2. Shuttle Radar Topography Mission (SRTM)

The SRTM elevation data are publicly available (http://srtm.csi.cgiar.org/) for a near-global scale at 3 arc sec (~90 m) spatial resolution with 16 m vertical accuracy (Farr and Kobrick, 2000). These data were obtained using the dual Space-borne Imaging Radar C-band (SIR-C) data with a wavelength of 5.6 cm, which is similar to Radarsat-1 in terms of its penetration ability of the dry sand to portray near surface features (Ghoneim and El-Baz, 2007b).

Over the last decade, the SRTM data were preferred for use in arid lands rather than other digital elevation data, such as the ASTER 30-m G-DEM. Although the SRTM data have coarser spatial resolution, they have proven to be more accurate in revealing the surface topography than DEMs from ASTER images, especially for drainage extraction in poorly vegetated areas (Pryde et al., 2007; Huggel et al., 2008). Moreover, DEMs from ASTER images have maximum errors of several hundred meters larger than those of the SRTM DEM (Kääb, 2005). The utilization of the SRTM data in this research was not only for the traditional usage of the drainage network delineation but also to model and simulate paleotopography.

The SRTM processing started by constructing a DEM mosaic to extract the watershed of Wadi El-Arish and its tributaries; five scenes of void-filled seamless SRTM images were utilized. The flow direction grid was extracted using ArcHydro tools based on the D8 flow direction algorithm (Jensen and Domingue, 1988), which is widely used in arid environments (e.g., Foody et al., 2004; Ghoneim, 2008; Ghoneim and Foody, 2013). The density of the drainage network was defined using an appropriate threshold of 500 cells of contributing drainage area (Fig. 3). Prior to performing the DEM simulation, a structural analysis was conducted to define the recent tectonic events that have influenced the geomorphologic evolution of Wadi El-Arish.

3.3. Structural analysis

In order to identify and map the former course of Wadi El-Arish, it was vital to initially define the obstacle that may have forced the stream to deviate from its original course. Therefore, we investigated the structural trends along Wadi El-Arish, particularly around the
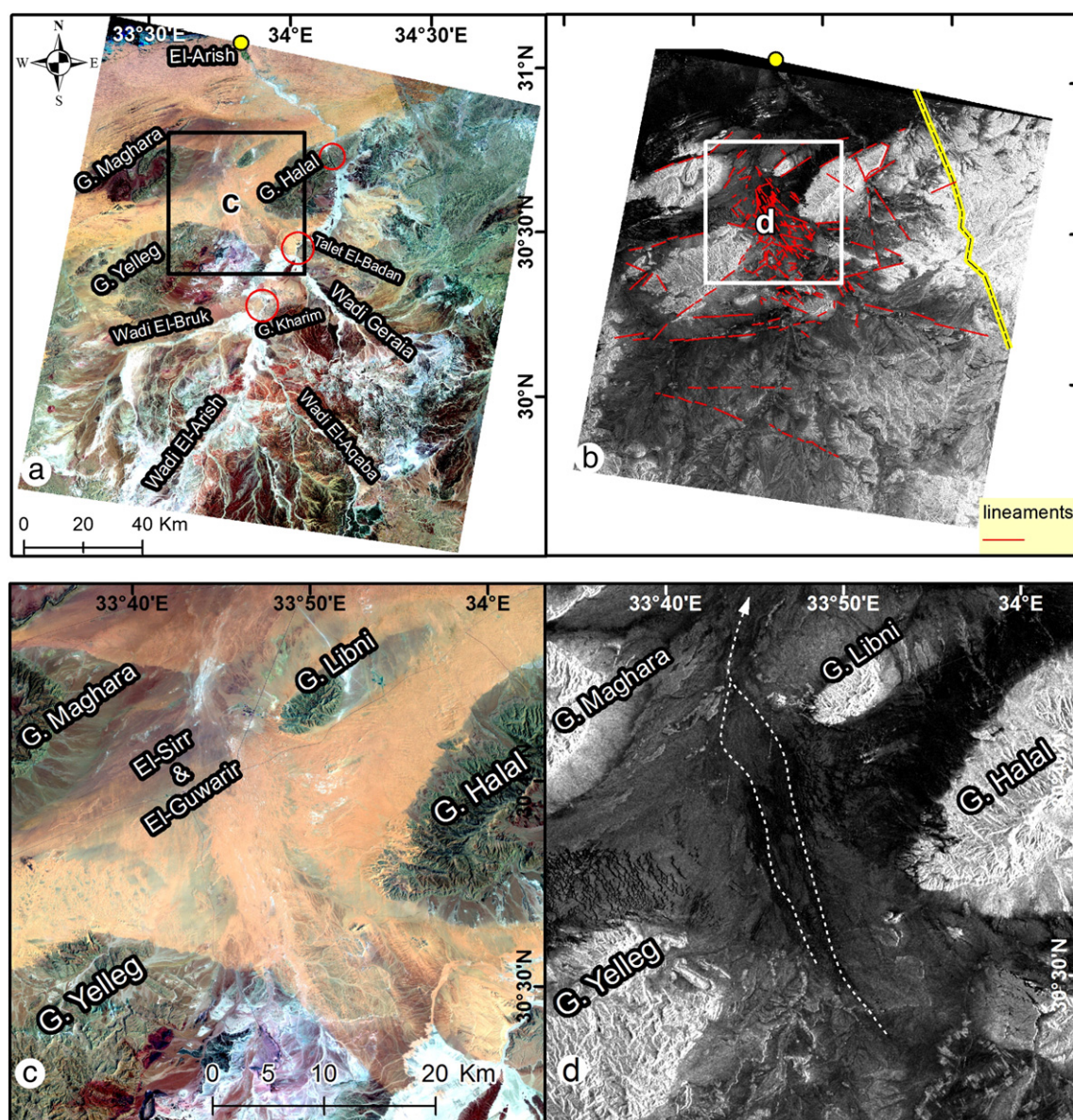
Fig. 2. Representation of the data sources. (a) Landsat ETM + color composite (bands 7, 4 and 2 as RGB) showing the tributaries of Wadi El-Arish in bright color of high albedo. The red circles mark the three gorges of Wadi El-Arish that incise into the folded ridges. The black box shows the location of (c). (b) Enhanced Radarsat-1 image showing the deduced subsurface lineaments. The white box demarks the location of (d). (c) Magnified view showing the area between the anticlinal hills of the Syrian Arc System, with no surface sign of a master drainage. (d) Magnified view revealing traces of two parallel tributaries trending northwest that join and point to northeast.

three gorges of Gebels Kharim, Talet El-Badan and Halal (Fig. 2a). The major surface and near-surface lineaments were manually-defined using the Radarsat-1 image (Fig. 2b) and the SRTM DEM derived hill-shade raster, respectively (Fig. 3). The deduced structural lineaments were combined with all folds and faults that were digitized from the Geological Map of Sinai (Klitzsch et al., 1987; Fig. 4a). The deduced lineaments include 31% more structures than that recognized in the map.

The accuracy of the lineament extraction from optical satellite images relies on the sensor characteristics, spatial and spectral resolution, and weather-illumination conditions (Smith and Wiseb, 2007). Hence, DEM-derived shaded relief was utilized, because it was proven to be a reliable alternative data source for lineaments and faults extraction (Hooper et al., 2003; Ganas et al., 2005). Manual detection was applied to the hill-shaded relief image and terrain spatial parameters derived from SRTM (e.g., aspect, gradient, and curvatures). The ER Mapper 7 software was used to trace the faults and lineaments because it allowed freehand control in the sunlight azimuth and altitude. Although manual detection is tedious and time-consuming, it has been chosen for its optimum accuracy in comparison to that of the automated extraction (e.g., Masoud and Koike, 2011). The generated lineaments were analyzed spatially and statistically using the zonal statistical tools in the ArcGIS 10.0 software. All lineaments were classified chronologically based on crosscutting and stratigraphic relationships to detect the recent fractures and active faults (Fig. 4a).

3.4. DEM simulation

A DEM simulation was developed to reconstruct the structural deformation and restore the paleotopography in order to better understand the evolution history of the paleodrainage (Fig. 4), and to validate the findings of the radar data. This technique incorporates the DEM data and the defined structural deformation to reconstruct the ancient terrain surface and allow the runoff to flow as it used to
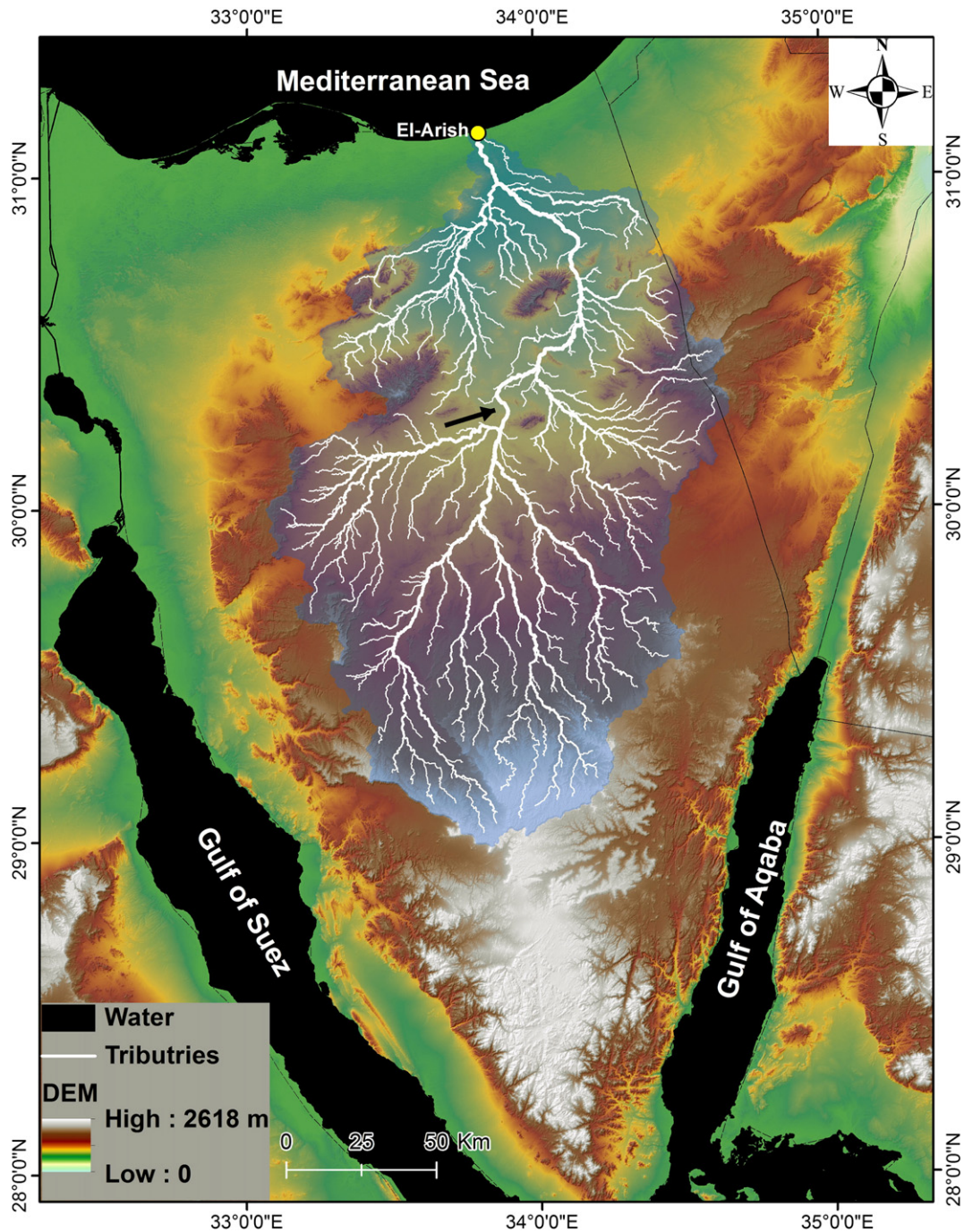
Fig. 3. Topography (SRTM DEM) of the Sinai Peninsula overlain with the extracted drainage network of Wadi El-Arish; channel lines within the watershed are shown in white. Streams of the first order are masked to enhance the appearance of the main channels. The black arrow points to the sharp bend (S-shape) in the master stream.

during pluvial periods. The simulation process was performed in MATLAB Ver. 2009b software in three main steps. First, the elevation of the suspected uplifted structure (anticlinal fold), which most likely blocked the former main channel course of Wadi El-Arish, was lowered to the surrounding topographic surface (Fig. 4d, e). Second, the two gorges of Gebels Talet El-Badan and Halal were raised, because they most probably were not formed during this stage. These DEM-modifications allowed the main course of Wadi El-Arish to flow northwest instead of northeast as it most likely did in the geologic past. Third, the DEM with the modified elevation was exported to the ArcHydro module in order to re-execute the automated drainage extraction process and simulate the former drainage network (Fig. 5).

4. Results and discussion

4.1. Mapping of the ancestral drainage course of Wadi El-Arish

The Radarsat-1 image reveals new previously unrecognized evidence for paleodrainage features along the ancestral course of Wadi El-Arish. It clearly shows, for the first time, visible segments of the buried ancestral course of Wadi El-Arish (Fig. 2d). The former course appears as a dark line of low radar backscatter, southwest of G. Halal. The drainage course splits into two parallel channels trending NW between G. Halal and G. Yelleg, and then converges into one channel in the area between Gebels Libni and El-Maghara (Fig. 2d). Areas of radar low backscatter are consistent with fine grained fluvial deposits
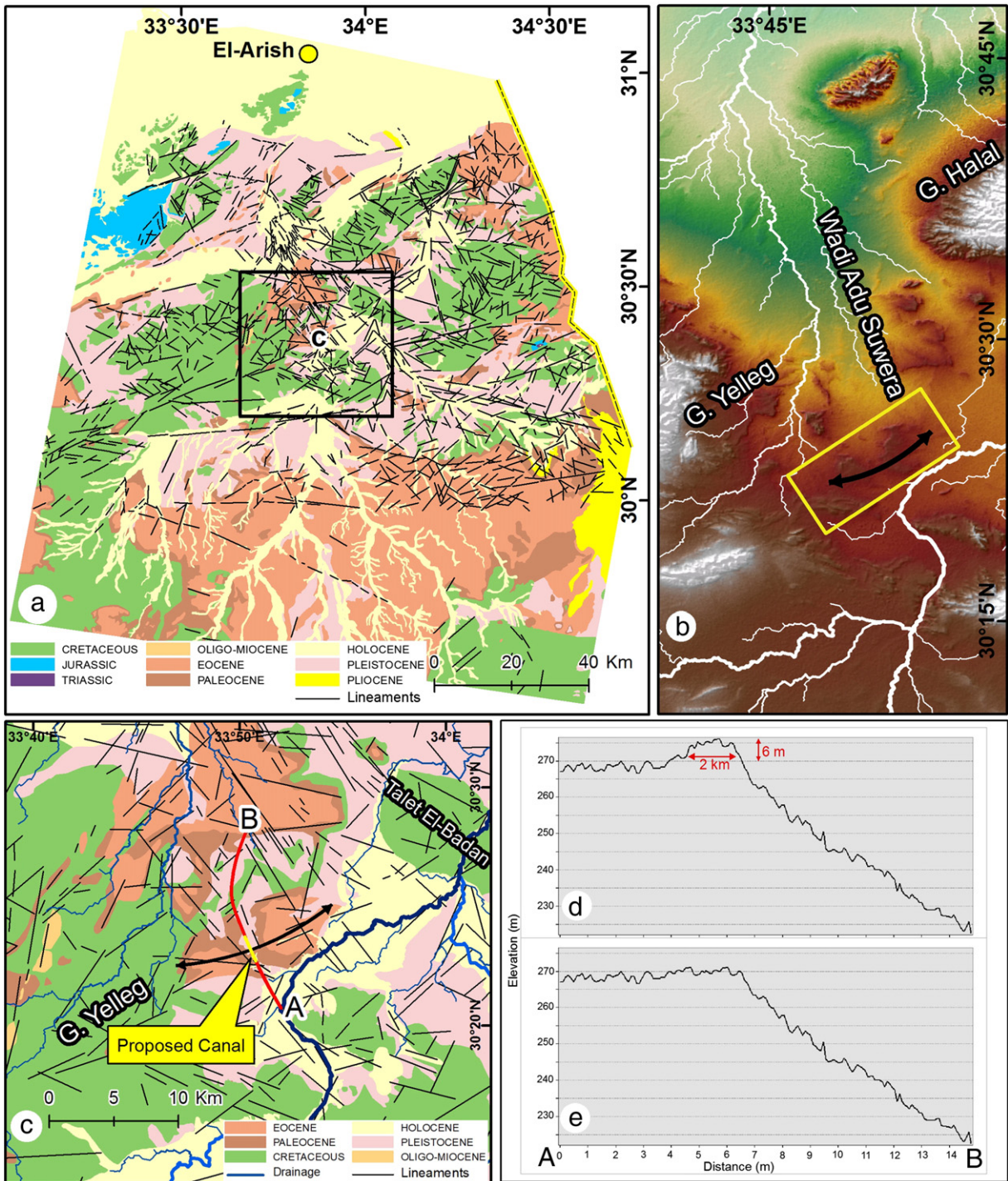
Fig. 4. Paleotopographic simulation of the ancestral channel of Wadi El-Arish. (a) Geological map of the study area with the DEM-derived lineaments. The black box shows the location of (c). (b) SRTM DEM to the SW of G. Halal with the drainage network. The yellow rectangle shows the location of the anticlinal fold of Wadi Abu Suwera that probably caused the deviation of the main course of Wadi El-Arish (see Fig. 5c). (c) Close view of the area east of G. Yelleg. The profile A–B in red follows the NW extensional fault and passes through the crest of an anticlinal fold, which has the same direction of the Syrian Arc System; the yellow segment denotes the proposed canal. Note that the Pleistocene deposits along the profile unconformably overlay the Eocene and Cretaceous rocks, indicating that the folding has occurred prior to Pleistocene deposits. (d) A–B profile derived from the SRTM data showing the present topography with a structural rise (ca. 6 m height and 2 km length). (e) A–B profile after lowering the topography, with the disappearance of the structural rise.

(Deroin et al., 1997). These likely formed at the end of the Neogene's humid phases when the climate changed to arid, and the rivers that drained from the highlands of central and south Sinai became less active. At present, these courses are mostly covered by a sand layer and are barely visible on the Landsat ETM+ (Fig. 2c), thus, remained unnoticed. The identification of this buried channel segment confirms the northwest direction of the former river course of Wadi El-Arish,

which was earlier proposed by El-Baz et al. (1998). Hence, the event that caused the change of the flow direction of Wadi El-Arish from NW to NE and resulted in the incision of narrow gorge at G. Halal should be carefully investigated.

The chronological sequence of the lineaments showed that the majority of the NW Quaternary fractures are restricted to the northern edge of the central carbonate plateau, between the largest
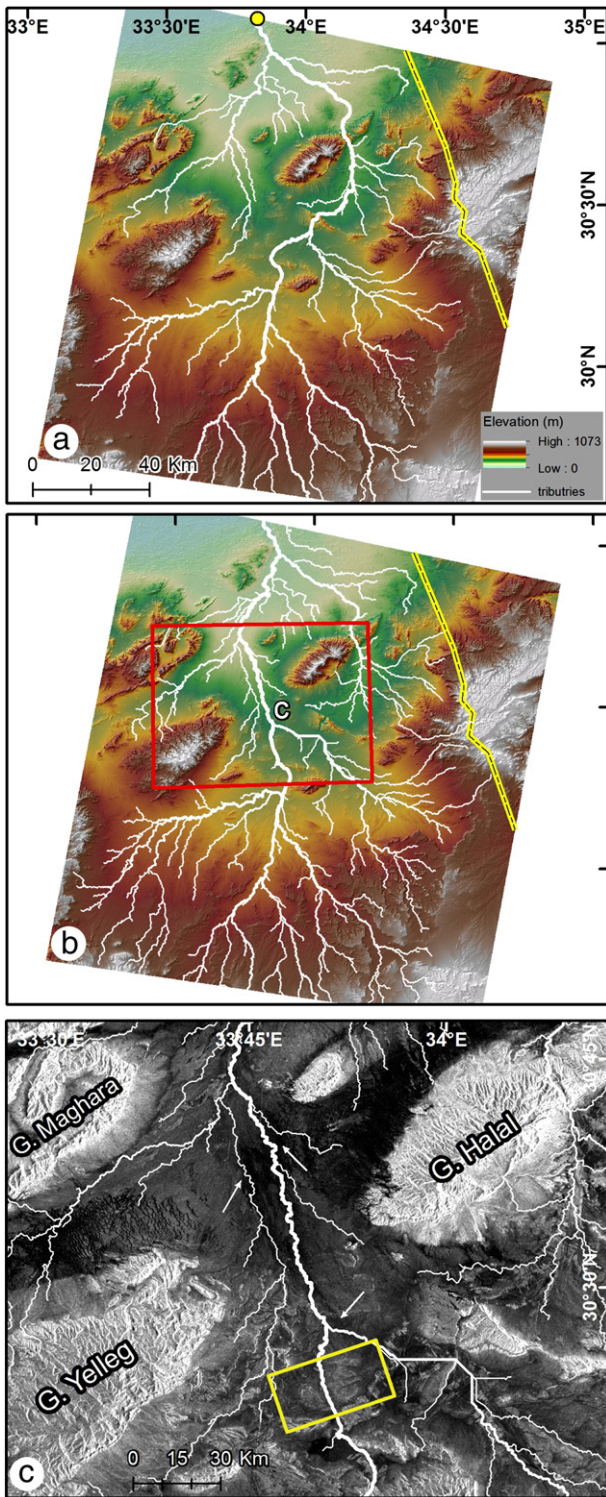
Fig. 5. Extraction of the ancestral channel of Wadi El-Arish from the modified DEM. (a) Extracted drainage network derived from the original DEM (before modification) showing the present course of the paleoriver. (b) Extracted drainage network derived from the modified DEM simulating the former course of Wadi El-Arish. The red box represents the area of (c). (c) Radarsat-1 image with the simulated drainage network. The white arrows point to the good matching between the extracted streams and the dark lines of the low backscatter. Compare with Fig. 2d.

anticlinal ridges of the Syrian Arc System (SAS), Gebels Halal and Talet El-Badan (Fig. 4a). This location contains structural uplift, herein referred to as Wadi Abu Suwera fold, and seems to be part of the

Syrian Arc Fold Belt, because it has the same axial trend of the SAS, NE direction (Fig. 4b). However, it is distinguished by the exposure of younger sediments (Eocene and Paleocene rocks), while the surrounding folds of Gebels Yelleg, Talet El-Badan and Halal have older exposed rock units of Cretaceous limestone (Fig. 4c). This could be a result of the recent uplifting of the SAS that has been documented (e.g., Kebeasy, 1990; Chaimov et al., 1992; Kusky and El-Baz, 2000), and the limited time for erosion processes to wear down the Eocene formations in comparison to the earlier folds. Furthermore, the extension of the lineaments through young and old deposits (Fig. 4c) suggests the recent uplift of the old anticline fold. In addition, the present shape of the main course of Wadi El-Arish has a sharp bend at the southern flank of the anticlinal fold of Wadi Abu Suwera (blade arrow in Fig. 3). The main drainage course abruptly changes its direction at this bend by 60°. Therefore, we propose that the structural highs of Wadi Abu Suwera may have blocked the main channel of Wadi El-Arish during the recent uplifting of the SAS and forced it to flow to the northeast.

The DEM simulation was utilized to modify the terrain of the area that was affected by the recent uplifting. Here, the altitude of the anticlinal fold of wadi Abu Suwera was lowered by ca. 6 m, from 276 to 270 m (Fig. 4d, c). This eliminates the effect of the post-Pleistocene uplift and allows the water to flow naturally as it used to during former humid phases (Fig. 5b). The DEM-simulated drainage validates the deduced NW drainage direction from the Radarsat-1 image of Wadi El-Arish. The extracted drainage network fits precisely on the low backscatter segment of the radar image (Fig. 5c). This inferred scenario of paleodrainage topography is consistent with the inferred two radar-dark linear features visible in the Radarsat-1 image west of G. Halal. The main channel of Wadi El-Arish appears as the eastern branch, while the western branch has lower stream order and drains from G. Maghara. The two channels merge at the junction between Gebels Maghara and Libni as shown on the SAR image (Fig. 2d). The radar-dark linear segment, visible on the Radarsat-1 image and the DEM-simulated drainage, reveals the former drainage course of Wadi El-Arish that is currently buried beneath the sand (Fig. 2c).

4.2. Paleolake development

The paleolakes of North Sinai were essentially developed in a vast structurally controlled depressions surrounded by the SAS ridges, which acted as natural dams for surface water during pluvial phases. These structurally controlled depressions were defined on the DEM, and integrated with the enhanced radar image to delineate the extent of the lacustrine deposits within the depressions. The formation of these paleolakes appears to have developed stage-wise and completed in two main stages separated by the uplifting and the deviation of the main river course, herein referred to as pre- and post-uplift stages (Fig. 6).

4.2.1. Pre-uplift stage
The initial stage of paleolake formation consisted of two phases. The first phase occurred during the early pluvial cycles of the Pleistocene, where several isolated paleolakes were formed south of G. Halal due to the excessive rainfall over the highlands of Central and Southern Sinai. At that time, the runoff probably did not have an exit to the Mediterranean Sea prior to the incision of the three gorges of the doubly plunging ridges of the SAS. Thus, the three gorges of Gebels Kharim, Talet El-Badan and Halal are assumed to be closed during the first phase of this stage. The first paleolake (herein referred to as PL1) was formed behind the anticlinal fold of G. Kharim, and extended longitudinally along the upper reaches of Wadi El-Arish and along Wadi El-Bruk southwest G. Kharim (Fig. 6a). The second lake (herein referred to as PL2) was formed behind (i.e., south of) the anticlinal fold of G. Talet El-Badan at the outlet of Wadi Geraia (Fig. 6a). During that period, Wadi El-Bruk seems to have been affected
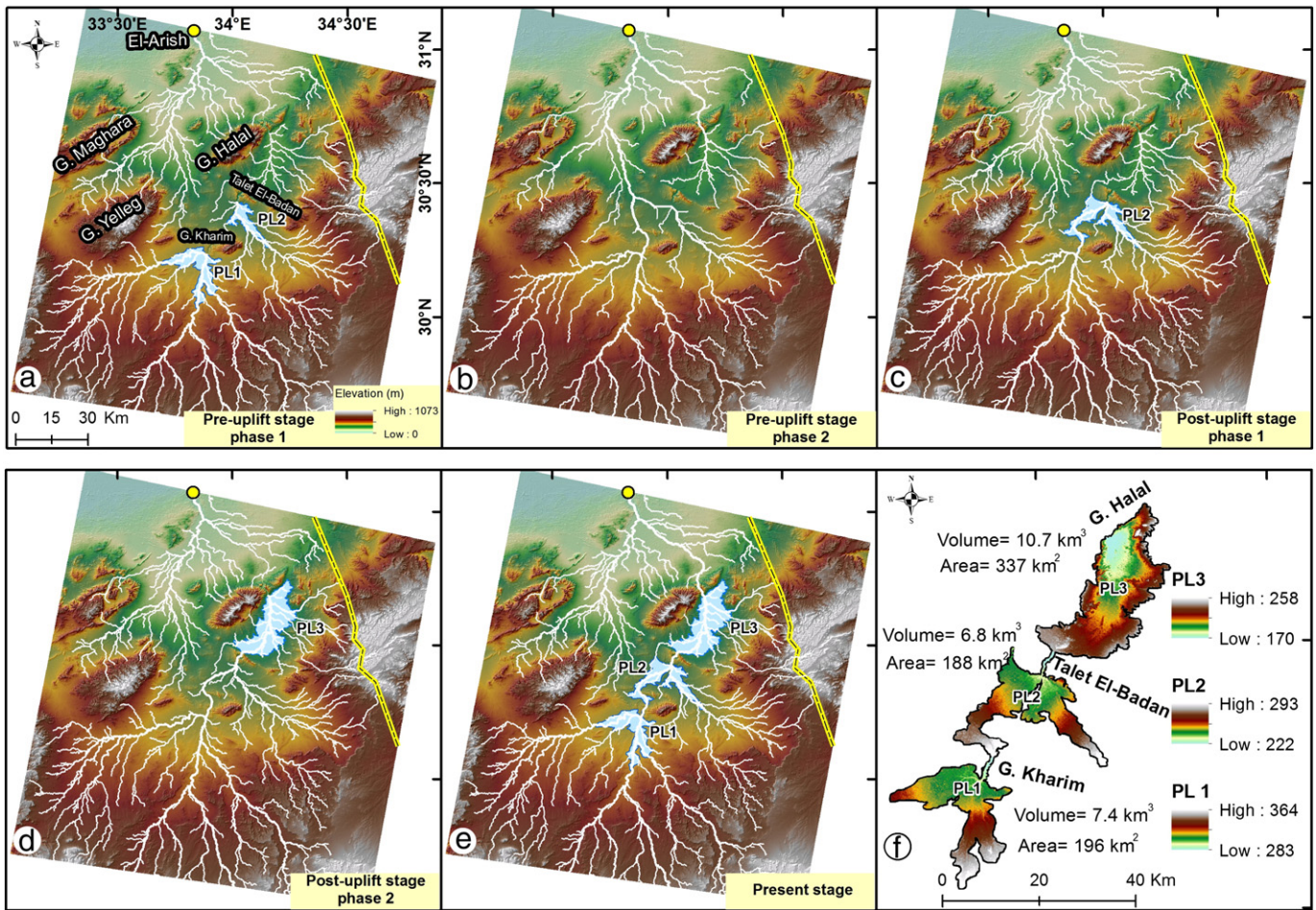
Fig. 6. Stages of paleolake development based on the simulated DEM. The drainage lines are shown in white and the paleolakes appear in light blue. (a) Initial stage of paleolake development showing the formation of the first paleolake (PL1). Note the early formation of PL2, at the outlet of Wadi Geraia. (b) Second phase of the pre-deviation stage showing the drainage network after it found a way to the Mediterranean Sea through the ancestral course of Wadi El-Arish. (c) Post-deviation stage, with the first phase showing the proposed scenario of the drainage system after the structural uplift blocked the former course and forced the main stream to deviate to NE. The second lake (PL2) developed behind G. Talet El-Badan during this stage. (d) Second phase of post-deviation stage demonstrating the shape of streams after the water broke through the gorge of Talet El-Badan and moved to the next topographic depression. The third lake (PL3) probably formed during this phase behind the anticlinal ridge of G. Halal. (e) The present shape of the simulated paleolakes within Wadi El-Arish. (f) DEM derived-SRTM showing the basins of the paleolakes with the estimated area and volume of each.

by stream piracy and its flow direction deviated from NNE to ENE, forming temporary paleolakes as indicated by deposits along its dry riverbed (Kusky and El-Baz, 2000).

In the second phase, the flood water filled the topographic depression of PL1, and spilled over northward into PL2. During this phase the runoff scoured the 45-m deep gorge of G. Kharim. Subsequently, the water level in PL2 increased and eventually the excess water found its way to the Mediterranean Sea through an NW flow direction between Gebels Halal and Yelleg (Fig. 6b). This led to the formation of the ancestral course of Wadi El-Arish, which was inferred from the SAR image. At present, this course and its tributaries are defunct, and barely visible in the optical images.

4.2.2. Post-uplift stage

During the first phase of this stage, the recent uplift of the SAS occurred in northern Sinai (Barazangi et al., 1996; Kusky and El-Baz, 2000) and resulted in an anticlinal fold rise at the entrance of Wadi Abu Suwera, east of G. Yelleg (Fig. 4b). This anticline blocked the course of Wadi El-Arish and forced its flow to deviate from NW to NE, leaving an S-shape on the present course (Fig. 3). The drainage network of the former course of Wadi El-Arish, west of G. Halal was continuing to receive a little amount of the flow from G. Yelleg and G. Halal (Fig. 6c).

In the second phase, the surface runoff began to accumulate in the closed depression of PL2, prior to the break of the gorge of Talet El-Badan. When the water level increased in PL2, the flood water incised several pathways around and through the gorge of Talet El-Badan and flowed toward a vast depression south of G. Halal. Ultimately, the overflow water formed the largest paleolake (herein referred to as PL3) at a structurally controlled depression south of G. Halal (Fig. 6d). During this phase, the three paleolakes (PL1, PL2 and PL3) were connected through gorges. However, they did not have an exit to the Mediterranean Sea (Fig. 6d). Some evidence of fresh water fauna and flora suggests that the paleolakes may have had significant residence time (Issar and Eckstein, 1969; Goldberg, 1984). Due to the large amount of floodwater received from the upper stream area and the surrounding highlands during the Holocene period, PL3 became the largest water body in northern Sinai with an area of 337 km^2 and a total water volume of about 10.7 km^3 (Fig. 6f). Overtime, the water of PL3 eroded the NW extensional fault of G. Halal and cut through a 200 m-deep gorge. The lake water then rushed through the gorge and flowed downstream toward the Mediterranean Sea. Finally, the water reached the sea in El-Arish City and the present course of Wadi El-Arish was established (Fig. 6e).

This hypothesis is supported by two lines of evidence: first, the presence of remnants of pluvial lake deposits within the basins of

the three identified paleolakes (e.g., Shata, 1959; Sneh, 1982; Issawi and Osman, 2008). Second, the width of the gorges increases from south to north, which indicates the chronological order of gorge formation (the oldest in the south, Fig. 2a). This evidence was confirmed during the field work by measuring the width of the gorges and examining the existing lacustrine deposits.

4.3. Fluvial deposits

Landsat ETM images show that most of the channels of Wadi El-Arish are covered by bright deposits of high albedo. Kusky and El-Baz (2000) suggested that these deposits are remnant sediments of dry lake beds formed during the fluvial phases. Accordingly, they assumed that the paleolakes were formed along the entire drainage course of Wadi El-Arish. However, these bright surface deposits represent soil enriched with clay minerals that most likely were deposited during the recent flash flood events as a result of occasional sporadic rainstorms. The broad channels of Wadi El-Arish allow the water to stagnate in the main tributaries and as the water evaporates and seeps into the soil, salts and clay minerals are left on the surface giving the bright color in the satellite images. Hence, we assume that the paleolakes were basically formed within the topographically low lands between anticlinal structures. This has been supported by the interpretation of the SAR image and field observations, which reveal thick terraces of lacustrine deposits and fresh water fauna within the depressions of PL1, PL2 and PL3 and SW of G. Halal (Sneh, 1982).

The age of the paleolake deposits in the study area is undefined precisely; it ranges from the Middle Palaeolithic (90,000–65,000 years B.P) as documented by Goldberg (1984) at southwest of G. Halal, to the Upper Palaeolithic (25,000–10,000 years B.P) as described by Bar-Yousef and Phillips (1977) at the southern flanks of G. Maghara. The archaeological evidence revealed by these authors suggests that the lacustrine deposits formed at ca. 13,500 years B.P. in lakes that could persist for about 100 years (Kusky and El-Baz, 2000). Therefore, we recommend further studies to precisely define the age of the paleolake deposits of Wadi El-Arish and other adjacent drainage systems at southern Sinai (e.g., Wadi Feiran) to understand the chronologic evolution of the paleodrainage system in the Sinai Peninsula.

4.4. Field validation

The field work for the present study was carried out on April 2012 to validate the proposed assumptions of the paleolakes and the paleochannel course of Wadi El-Arish. Field investigations included measuring the thicknesses of lacustrine deposits in three sites along the assumed paleolakes locations. The investigations extended to cover the site of the ancestral course of Wadi El-Arish that was inferred from the low radar backscatter of the SAR image.

4.4.1. Lacustrine deposits at paleolake sites

The folded ridges of North Sinai appear to have a direct influence on the formation of the lacustrine deposits along Wadi El-Arish. In most cases the lacustrine terraces are located in topographic depressions bordered by highlands of the folded SAS (Fig. 7a, c). Two types of lacustrine deposits were identified along the main channel of Wadi El-Arish. The first type is composed mainly of consolidated sand and located at the borders of the paleolake sites of PL1, PL2 and PL3. The largest thickness of these deposits was measured south of G. Halal on the western banks of PL3 with a thickness of 5–7 m above the wadi floor (Fig. 7a) that furnished with particles of limestone and very coarse gravel (32–64 mm). The thickness of the lacustrine deposits indicates that they were not formed within ephemeral rivers such as the present ones. Rather, they probably formed during the past fluvial periods. The second type of lacustrine

deposits is composed of silt and very fine sand, and situated in the open wadi channels in the form of continuous terraces along the entrances and the exits of the gorges. Remnants of these terrace deposits at the gorge outlet of G. Halal (Fig. 7b) have an average thickness of 2 m. This lacustrine bed extends for about 500 m along the western bank of the main stream course of Wadi El-Arish, north of the gorge of Halal. In floodplain areas, recent lacustrine deposits have been redistributed and used for seasonal agriculture activities after flash flood events (Fig. 7d). Such agricultural use indicates the fertility of these deposits that could be used for sustainable agricultural development, especially with an improved management strategy of water resources.

The paleolakes of Wadi El-Arish occupy vast areas and are covered with a flat bright surface of silt and clay, mixed with salts and very fine sand deposits, and often exhibit by mud-cracked patterns (Fig. 7e). The shape, composition and geometry of these broad areas suggest that they are dry lake beds formed essentially during the past fluvial phases, and extended to cover the foothills of the highlands. When the climate became dry, the shoreline of these paleolakes regressed to the center of the depressions, leaving fluvial deposits of well sorted pebbles and granules on the lake beaches (Fig. 7f). At present, the occasional flash floods restore and maintain the paleolake bed (lacustrine deposits) by enriching the soil cover with wadi wash deposits (Fig. 7f). These immense paleolakes could be optimum lands for agricultural development in North Sinai, provided that sustains a source of water with appropriate flood mitigation. However, because the last cycle of the wet periods ended at about 5.5 ka in the Sahara (Szabo et al., 1995; De Menocal et al., 2000), the shoreline and the sites of these paleolakes should be carefully surveyed for the potential uncovering archaeological sites of human, animals or plant remains prior to any development plan.

4.4.2. Fluvial deposits at the ancestral course site

The interpretation of the radar image was in desperate need of field confirmation to support the paleochannel course assumptions. For that end, a site was chosen for field investigation located on the dark line of low radar backscatter, which represents the former course of Wadi El-Arish west of G. Halal (Fig. 8a). That site is located in the northern part of the El-Sirr and El-Guwarir areas (Fig. 2c), southwest G. Libni, and is surrounded by sand dunes cut by channels of fluvial deposits (Fig. 8c). A surface layer of salts mixed with silt, clay and fine sands was observed at the end of these channels where they were blocked by sand dunes (Fig. 8b). Although this salt layer has the bright spectral reflectance of the broad lake deposits, it is barely visible in the Landsat ETM + (~30 m) image, because of the limited exposure between the sand dunes and their discontinuous nature (Fig. 8d). The salt layer probably indicates that these channels were filled with water during humid periods before they became dry due to the local uplift that blocked the water flow from upstream. The residual water in the channels evaporated, while salts and very fine fluvial deposits remained on the surface. These deposits were interpreted on the SAR image as a line of low radar backscatter. During dry climate, such as the present one, the fluvial deposits were exposed to wind action, and re-shaped into dunes and sand sheets. The prevailing wind direction eroded the salt layer and redistributed the sands over the fluvial deposits (Fig. 8d). These deposits, therefore, are more visible on SAR images rather than optical ones. This hypothesis was first developed to explain the origin of the sand dunes in the Western Desert of Egypt (El-Baz, 1992). Hence, it is logical to assume that the sand dunes in the El-Sirr and El-Guwarir areas could be of fluvial origin (Fig. 8c). These dunes, most likely, did not contribute to the blocking of the old river course of Wadi El-Arish. Sand dunes might only hinder the flow in channels if water flow became very rare, or the aeolian sand supply exceeds the transport ability of the drainage (Kusky and El-Baz, 2000).
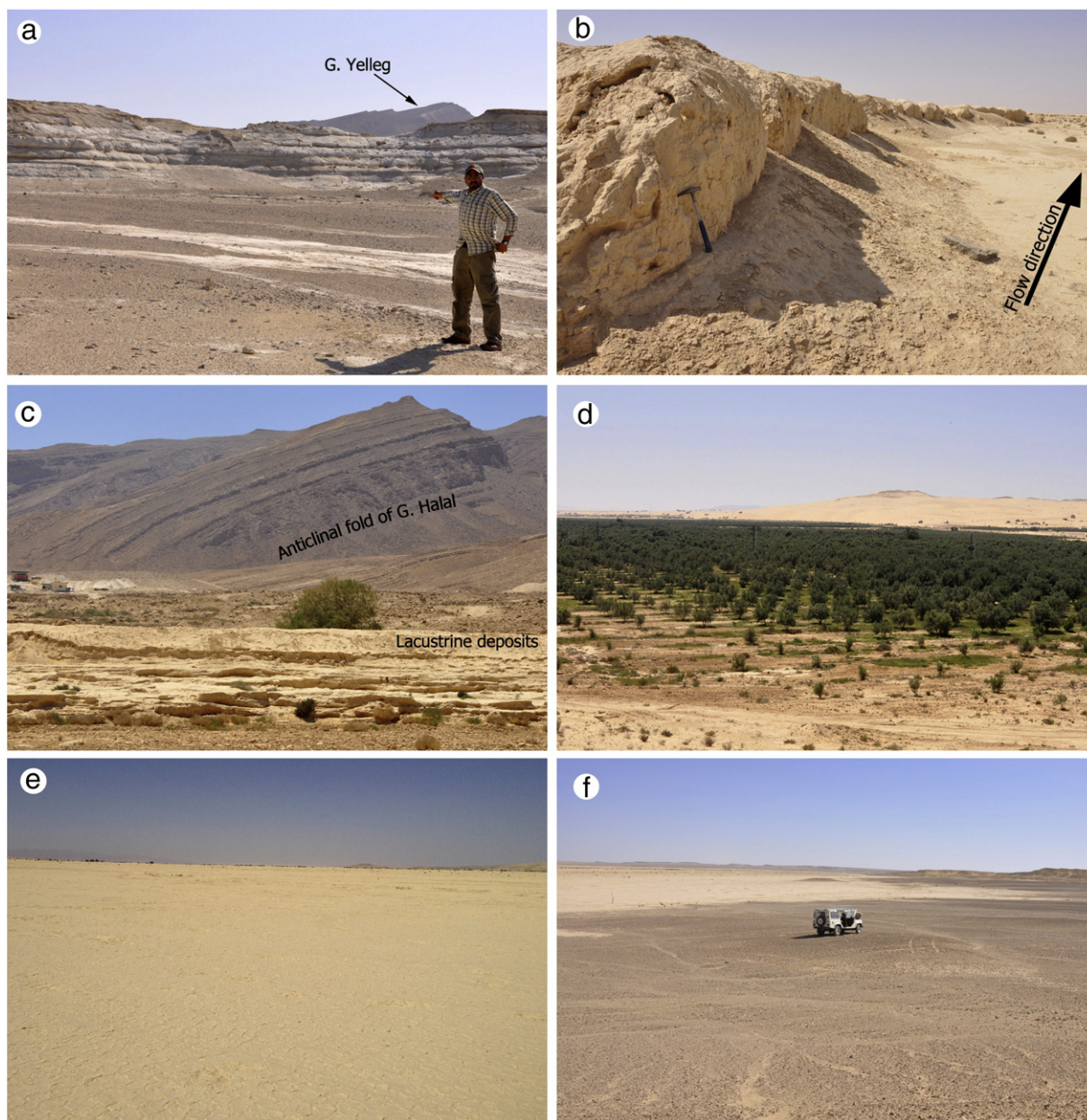
Fig. 7. Field photographs of the lacustrine deposits. (a) Remnants of the fluvial-lacustrine deposits south of G. Talet El-Badan with an average thickness of 5 m. Note the folded ridge of G. Yelleg in the background. (b) Extension of the fluvial terraces at the outlet of G. Halal Gorge. (c) Lacustrine deposits at the site of PL3 bordered by the western flank of the anticlinal fold of G. Halal in the background. (d) Cultivated lands on fluvial deposits at the downstream of Wadi El-Arish indicating the suitability of the soil for agricultural activities. (e) Broad extent of the paleolake surface in Wadi El-Arish; note the mudcrack patterns on the surface and the bright color of the soil, which appears as high spectral reflectance in Landsat images (see Fig. 2a). (f) Present shoreline of paleolake (PL2) between the old fluvial deposits, where the Jeep is situated, and the young alluvial deposits of Wadi El-Arish, in a bright color.

4.5. Implications to groundwater accumulation

Although Wadi El-Arish is an ephemeral drainage, its former course and the three paleolake basins along its present course could contain a considerable amount of groundwater at various depths. The development of the paleolakes within structurally-controlled depressions increases the possibility of fracture zone aquifers (Wright and Burgess, 1992). During pluvial periods, a significant amount of the lake water would have infiltrated and recharged the underlying substrata through the dense network of fractures in the carbonate rocks (El-Baz et al., 1998). Such water is most likely preserved beneath the paleolakes within the Tertiary carbonates and porous Pre-Tertiary sandstone formations.

The later structural uplifting in the region folded the Paleocene and Oligo-Miocene shale (Said, 1990), and formed aquicludes that prevented the lateral migration of groundwater. The present gorges of Wadi El-Arish slow down the flow of the seasonal floodwater and cause frequent formation of temporary lakes within the paleolake basins. Some of this temporary water would seep and recharge the local Quaternary aquifers. Thus, such lake beds could host a large amount of groundwater (both fossil and renewable), which is of great importance to the future development in the study region.

Although Wadi El-Arish is one of the widest ephemeral streams in Egypt (5–8 km wide behind the gorges), sporadic flash flood events threaten the efforts to establish agricultural development along its course. This study suggests an alternative area for sustainable
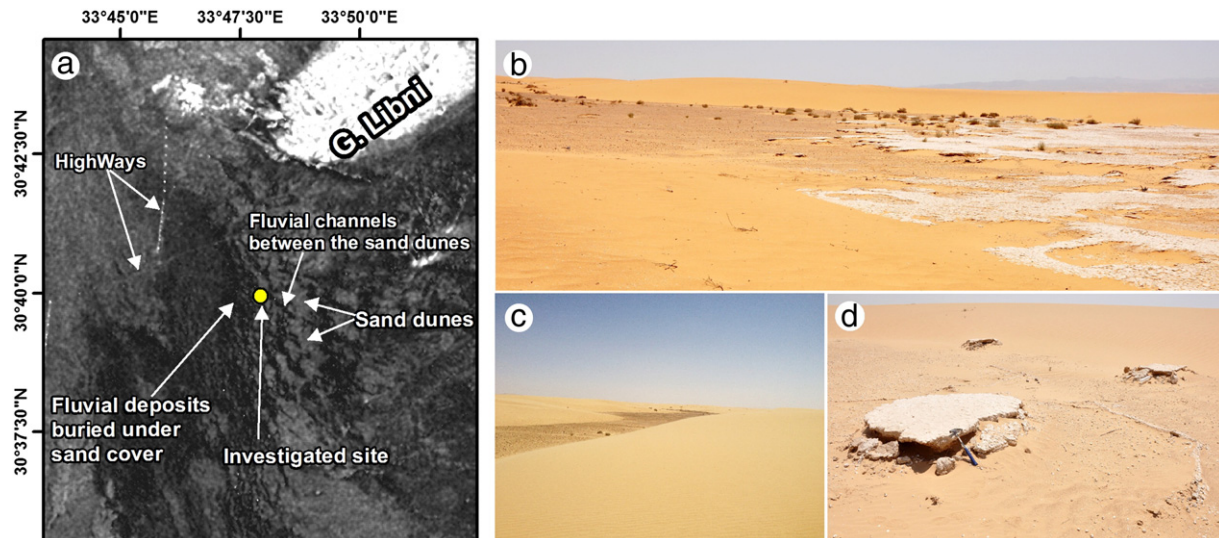
Fig. 8. Field explanations of the fluvial deposits at the ancestral course site. (a) Radarsat-1 image showing the visited site at the assumed location of the ancestral course of Wadi El-Arish. It distinguishes the radar backscatter into the predominant land features based on field confirmation. (b) Example of a fluvial paleochannel between sand dunes. The white salt layer at the end of the channel indicates the evaporation result of the stagnant water along the paleostream. It also demonstrates the dark line of low radar backscatter. (c) Extension of a paleochannel course among sand dunes west of G. Halal. (d) Outcrops of the salt layer within the sand fields illustrating erosion of the surface.

development based on the new findings of the SAR data. The proposed area is surrounded by the three hills of G. Halal, G. Yelleg and G. Maghara, at the region of El-Sirr and El-Guwarir (Fig. 2c). This site contains the former course of Wadi El-Arish, as established by this study, and represents a promising area for agricultural development. In addition, the area has a considerable amount of Esna shale deposits, which consist mainly of claystone that is ideal for agricultural purposes (Temraz, 2010). Moreover, the early Cretaceous deep groundwater aquifer in the same area (Nubian Sandstone) has been brought close to the surface by the anticlinal folding of the surrounding hills (Hammad, 1980).

Based on the above, we propose to dredge a 2 km long channel with a depth of 6 m through the anticlinal fold of Wadi Abu Suwera in order to reconnect the present course of Wadi El-Arish to its former drainage course (Fig. 4c). This canal could be used to redirect the runoff of the upstream reaches to the proposed area of El-Sirr and El-Guwarir through the ancestral drainage course. This would result in creating approximately 1400 km^2 of fertile lands for sustainable development. However, the groundwater availability and quality in the proposed site should be carefully investigated before the canal dredging is approved, although the groundwater of the proposed area is probably of low salinity (Rosenthal et al., 2007). The average groundwater salinity during 1997–2011, obtained by the Water Resources Research Institute in El-Arish, shows a significant increase toward the NE (from 1600 ppm in Nakhl City to 3800 ppm at G. Kharim, and 4500 ppm at G. Halal), but a critical decrease toward the NW (~2800 ppm at El-Hasana Well, nearby the proposed area of development) (WRRI personal communication). Such a salinity distribution could be attributed to the presence of NW subsurface fractures that would act as hydraulic conduits and transfer percolated rainwater to repeatedly recharge the aquifers of the El-Sirr and El-Guwarir areas.

The proposed change of the flow direction, as a result of the canal establishment, will not affect the present stream segment in the eastern side of G. Halal, because Wadi Geraia will continue to flow through the present course of Wadi El-Arish to irrigate the reclaimed lands and maintain the water table in the wells. The proposed channel most probably will help in minimizing the flash flood risk and provide better exploitation of surface runoff that would otherwise be lost to the Sea.

5. Conclusions

This paper summarizes the geomorphic evolution of the paleodrainage and paleolakes in North Sinai. The ancestral course of Wadi El-Arish has been mapped by integrating a Radarsat-1 image with SRTM data in synergy with optical images and field investigations. With a length of 109 km and a width of 0.5–3 km, a segment of the former drainage course has been depicted for the first time beneath the windblown deposits west of G. (Gabel) Halal. Our data analysis indicated that the former course of Wadi El-Arish was dammed as a result of recent structural uplifting (anticlinal fold) at Wadi Abu Suwera. This structural high blocked the NW pathway, and forced the flow direction to deviate to the NE through the gorges of Talet El-Badan and G. Halal, respectively. A DEM-based simulation was employed to reconstruct the structural deformation and depict the paleodrainage history. The simulated drainages were matched with regions of low radar backscatter, validating the radar image interpretation. In addition, field investigations confirmed the presence of paleochannels filled with fluvial deposits and a salt layer partially covered by sand.

Three major paleolakes have been identified along the main course of Wadi El-Arish within structurally controlled depressions formed due to the anticlinal ridges of the Syrian Arc System in North Sinai. These paleolakes were most likely developed behind the folded hills in two main stages, interrupted by the deviation of the river course. During the first stage, the southern paleolake was developed from the excess rainfall of the upper reaches of Wadi El-Arish, where the river was probably blocked and failed to reach the Mediterranean Sea. The central and northern paleolakes were formed in the post-deviation stage, and the latter is estimated to be the largest of the three paleolakes (about 337 km^2).

The region in between Gebels Halal, Yelleg and El-Maghara represents a promising area for agriculture development with considerable amounts of surface clay minerals supplied from the Esna shale deposits. Moreover, this area contains relatively low groundwater salinity, and the deep groundwater aquifer of the early Cretaceous Nubian Sandstone has been brought close to the surface by anticlinal folding. We propose to establish a canal to reconnect the present drainage course with the former one, to redirect the occasional runoff to the vast flat fertile lands for sustainable agriculture and development in the region.

Acknowledgments

Appendix A. Supplementary data

Supplementary data associated with this article can be found in the online version, at http://dx.doi.org/10.1016/j.geomorph.2013.04.005. These data include Google map of the most important areas described in this article.

References

Abubakr, M., Ghoneim, E., El-Baz, F., Zeineldin, M., Zeid, S., 2010. Remote sensing data integration and runoff modeling to estimate flash flood in El-Arish, Sinai, Egypt. Geological Society of America, Abstracts with Programs 42 (5), 316.

Ambraseys, N.N., Barazangi, M., 1989. The 1759 earthquake in the Bekaa Valley: implications for earthquake hazard assessment in the eastern Mediterranean region. Journal of Geophysical Research 94, 4007–4013.

Barazangi, M., Fielding, E., Isacks, B., Seber, D., 1996. Geophysical and geological databases and GTBT monitoring: a case study of the Middle East. In: Huseby, E.S., Dainty, A.M. (Eds.), Monitoring a Comprehensive Test Ban Treaty. Kluwer Academic Publishers, Amsterdam, pp. 197–224.

Bar-Yousef, O., Phillips, J.L., 1977. Prehistoric investigations in Gebel Maghara, Northern Sinai. Chapter 2: Past and Present Environment. Qedem 7. Institute of Archeology, Hebrew University, Jerusalem, pp. 11–31.

Bosworth, W., Guiraud, R., Kessler, L.G., 1999. Late Cretaceous (ca. 84 Ma) compressive deformation of the stable platform of northeast Africa (Egypt): far-field stress effects of the "Santonian event" and origin of the Syrian arc deformation belt. Geology 27, 633–636.

Chaimov, T.A., Barazangr, M., Al-Saad, D., Sawaf, T., Gebran, A., 1992. Mesozoic and Cenozoic deformation inferred from seismic stratigraphy in the southwestern intracontinental Palmyride fold–thrust belt, Syria. Geological Society of America Bulletin 104, 704–715.

De Menocal, P., Ortiz, J., Guilderson, T., Adkins, J., Sarnthein, M., Baker, L., Yarusinsky, M., 2000. Abrupt onset and termination of the African Humid Period: rapid climate responses to gradual insolation forcing. Quaternary Science Reviews 19, 347–361.

Deroin, J.P., Company, A., Simonin, A., 1997. An empirical model for interpreting the relationship between backscattering and arid land surface roughness as seen with the SAR. IEEE Transactions on Geoscience and Remote Sensing 35, 86–92.

Diab, M.Sh., Himida, I.H., 1981. Water quality under Sinai Peninsula "Egypt". Studies in Environmental Science 17, 665–669.

El-Baz, F., 1992. In: Sadek, A. (Ed.), Origin and evolution of sand seas in the Great Sahara and implications to petroleum and groundwater exploration. Geology of the Arab World, vol. II. Cairo University Press, Cairo, pp. 3–17.

El-Baz, F., Kusky, T.M., Himida, I., Abdel-Mogheeth, S., 1998. Ground Water Potential of the Sinai Peninsula, Egypt. Ministry of Agriculture and Land Reclamation, Cairo (219 pp.).

El-Ghazawi, M.M., 1989. Hydrogeological studies in Northeast Sinai, Egypt. (Ph.D. Thesis) Geol. Dept., Fac. Sci., Mansoura Univ., Egypt (290 pp.).

Farr, T.G., Kobrick, M., 2000. Shuttle radar topography mission produces a wealth of data. EOS transactions. American Geophysical Union 81, 583–585.

Foody, G., Ghoneim, E., Arnell, N., 2004. Predicting locations sensitive to flash flooding in an arid environment. Journal of Hydrology 292, 48–58.

Ganas, A., Pavlides, S., Karastathis, V., 2005. DEM-based morphometry of range-front escarpments in Attica, central Greece, and its relation to fault slip rates. Geomorphology 65, 301–319.

Ghoneim, E., 2008. Optimum groundwater locations in the northern United Arab Emirates. International Journal of Remote Sensing 29, 5879–5906.

Ghoneim, E., El-Baz, F., 2007a. The application of radar topographic data to mapping of a mega-paleodrainage in the Eastern Sahara. Journal of Arid Environments 69, 658–675.

Ghoneim, E., El-Baz, F., 2007b. Dem-optical-radar data integration for paleo-hydrological mapping in the northern Darfur, Sudan: implication for groundwater exploration. International Journal of Remote Sensing 28, 5001–5018.

Ghoneim, E., Foody, G., 2013. Assessing flash flood hazard in an arid mountainous region. Arabian Journal of Geosciences 6, 1191–1202.

Ghoneim, E., Benedetti, M., El-Baz, F., 2012. An integrated remote sensing and GIS analysis of the Kufrah Paleorivers, Eastern Sahara. Geomorphology 139, 242–257.

Goldberg, P., 1984. Late Quaternary history of Qadesh Barnea, northeastern Sinai. Zeitschrift für Geomorphologie 28, 193–217.

Hammad, A., 1980. Geomorphical and hydrological aspects of Sinai Peninsula, A.R.E. Annals of the Geological Society of Egypt 10, 807–817.

Holbrook, J., Schumm, S.A., 1999. Geomorphic and sedimentary response of rivers to tectonic deformation: a brief review and critique of a tool for recognizing subtle epeirogenic deformation in modern and ancient settings. Tectonophysics 305, 287–306.

Hooper, D.M., Bursik, M.I., Webb, F.H., 2003. Application of high-resolution, interferometric DEMs to geomorphic studies of fault scarps, Fish Lake Valley, Nevada-California, USA. Remote Sensing of Environment 84, 255–267.

Huggel, C., Schneider, D., Miranda, P., Granados, H., Kääb, A., 2008. Evaluation of ASTER and SRTM DEM data for lahar modeling: a case study on lahars from Popocatépetl Volcano, Mexico. Journal of Volcanology and Geothermal Research 170, 99–110.

Issar, A., Eckstein, Y., 1969. The lacustrine beds of Wadi Feiran, Sinai: their origin and significance. Israel Journal of Earth Sciences 18, 21–27.

Issawi, B., Osman, R., 2008. Egypt during the Cenozoic: geological history of the Nile River. Bulletin of the Tethys Geological Society, Cairo 3, 43–62.

Jenkins, D.A., 1990. North and Central Sinai. In: Said, R. (Ed.), The Geology of Egypt. A.A. Balkema, Rotterdam, pp. 361–380.

Jensen, J.R., 2000. Remote Sensing of the Environment: An Earth Resource Perspective. Prentice-Hall, Englewood Cliffs, New Jersey (544 pp.).

Jensen, S.K., Domingue, J.O., 1988. Extracting topographic structure from digital elevation model data for geographic information system analysis. Photogrammetric Engineering and Remote Sensing 54, 1593–1600.

Kääb, A., 2005. Combination of SRTM3 and repeat ASTER data for deriving alpine glacier flow velocities in the Bhutan Himalaya. Remote Sensing of Environment 94, 463–474.

Kebeasy, R.M., 1990. Seismicity, chapter 5. In: Said, R. (Ed.), The Geology of Egypt. Balkema, Rotterdam, pp. 51–59.

Klitzsch, E., List, F.K., Pohlmann, G., 1987. Geological map of Egypt, North Sinai sheet. Scale 1,500,000. T.E.G.P. Corporation/Conoco, Cairo, Egypt.

Krenkel, E., 1925. Geologie der Erde, Geologie Afrikas. Gebrüder Borntraeger, Berlin (46 1 pp.).

Kusky, T.M., El-Baz, F., 1998. Structural and tectonic evolution of the Sinai Peninsula, using Landsat data: implications for ground water exploration. Egyptian Journal of Remote Sensing and Space Sciences 1, 69–100.

Kusky, T.M., El-Baz, F., 2000. Neotectonics and fluvial geomorphology of the Northern Sinai Peninsula. Journal of African Earth Sciences 31, 213–235.

Le Pichon, X., Gaulier, J.M., 1988. The rotation of Arabia and the Levant fault system. Tectonophysics 153, 271–294.

Lee, H., Chae, H., Cho, S., 2011. Radar backscattering of intertidal mudflats observed by Radarsat-1 SAR images and ground-based scatterometer experiments. IEEE Transactions on Geoscience and Remote Sensing 49, 1701–1711.

Masoud, A., Koike, K., 2011. Morphotectonics inferred from the analysis of topographic lineaments auto-detected from DEMs: application and validation for the Sinai Peninsula, Egypt. Journal of Tectonophysics 510, 291–308.

McCauley, J.F., Schaber, G.G., Breed, C.S., Grolier, M.J., Haynes, C.V., Issawi, B., Elachi, C., Blom, R., 1982. Subsurface valleys and geoarchaeology of the Eastern Sahara revealed by Shuttle Radar. Science 218, 1004–1020.

Mills, A.C., Shata, A., 1989. Groundwater assessment of Sinai. Egypt. Groundwater 27, 793–801.

Paillou, A., Schuster, M., Tooth, T., Farr, T., Rosenqvist, A., Lopez, S., Malezieux, J., 2009. Mapping of a major paleodrainage system in eastern Libya using orbital imaging radar: the Kufrah River. Earth and Planetary Science Letters 277, 327–333.

Parashar, S., Langham, E., McNally, J., Ahmed, S., 1993. Radarsat mission requirements and concepts. Canadian Journal of Remote Sensing 19, 280–288.

Pryde, J., Osorio, J., Wolfe, M., Heatwole, C., Benham, B., Cárdenas, A., 2007. Comparison of watershed boundaries derived from SRTM and ASTER digital elevation datasets and from a digitized topographic map. ASABE Paper No. 072093, St. Joseph, Michigan, USA.

Robinson, C., El-Baz, F., Al-Saud, T., Jeon, S., 2006. Use of radar data to delineate paleodrainage leading to the Kufra Oasis in the eastern Sahara. Journal of African Earth Sciences 44, 229–240.

Rosenthal, E., Zilberbrand, M., Livshitz, Y., 2007. The hydrochemical evolution of brackish groundwater in central and northern Sinai (Egypt) and in the western Negev. Journal of Hydrology 337, 294–314.

Said, R., 1990. The Geology of Egypt. A.A. Balkema, Rotterdam, Brookfield.

Schaber, G.G., McCauley, J.F., Breed, C.S., 1997. The use of multifrequency and polarimetric SIR-C/X-SAR data in geologic studies of Bir Safsaf, Egypt. Remote Sensing of Environment 59, 337–363.

Shata, A., 1959. Ground water and geomorphology of the northern sector of Wadi El-Arish basin. Bulletin of the society of Geography of Egypt 32, 247–262.

Shata, A., 1960. The geology and geomorphology of El-Qusayima area, Northeast Sinai, Egypt. Bulletin of the society of Geography of Egypt 33, 55–146.

Smith, M.J., Wiseb, S.M., 2007. Problems of bias in mapping linear landforms from satellite imagery. International Journal of Applied Earth Observation and Geoinformation 9, 65–78.

Smith, S., El-Shamy, I., Abd-El Monsef, H., 1997. Locating regions of high probability for groundwater in the Wadi El-Arish Basin, Sinai, Egypt. Journal of African Earth Sciences 25, 253–262.

Sneh, A., 1982. Drainage systems of the Quaternary in northern Sinai with emphasis on Wadi El-Arish. Zeitschrift für Geomorphologie 26, 179–185.

Sultan, M., Metwally, S., Milewski, A., Becker, D., Ahmeda, M., Sauck, W., Soliman, F., Sturchio, N., Yane, E., Rashed, M., Wagdy, A., Becker, R., Welton, B., 2011. Modern recharge to fossil aquifers: geochemical, geophysical, and modeling constraints. Journal of Hydrology 403, 14–24.

Szabo, B., Haynes, C., Maxwell, T., 1995. Ages of Quaternary pluvial episodes determined by uranium-series and radiocarbon dating of lacustrine deposits of eastern Sahara. Palaeogeography, Palaeoclimatology, Palaeoecology 113, 227–242.

Temraz, M., 2010. Mineralogical and geochemical evaluation of late Eocene shale Northern Sinai, Egypt. Journal of Petroleum Science and Engineering 75, 234–239.

Wright, E.P., Burgess, W.G., 1992. The hydrogeology of crystalline basement aquifers in Africa. Geological Society London, Special Publication 66 (264 pp.).

Youssef, M.I., 1968. Structural pattern of Egypt and its interpretation. American Association of Petroleum Geologists Bulletin 52, 601–614.